Published in final edited form as:
*J Vasc Surg*. 2012 August ; 56(2): 455–461. doi:10.1016/j.jvs.2012.01.038.

# Accelerated Aneurysmal Dilation Associated with Apoptosis and Inflammation in a Newly Developed Calcium Phosphate Rodent Abdominal Aortic Aneurysm Model

**Dai Yamanouchi**[*], **Stephanie Morgan**[*], **Colin Stair**, **Stephen Seedial**, **Justin Lengfeld**, **K. Craig Kent**, and **Bo Liu**[†]
Division of Vascular Surgery, Department of Surgery, University of Wisconsin School of Medicine and Public Health, 600 Highland Avenue, Madison, WI 53792

## Abstract

**Objective—**The Calcium Chloride ($CaCl_2$) model is a widely accepted rodent model for abdominal aortic aneurysm (AAA). Calcium deposition, mainly consisting of calcium phosphate ($CaPO_4$) crystals, has been reported to exist in both human and experimental aneurysms. $CaPO_4$ crystal has been utilized for in vitro DNA transfection by mixing $CaCl_2$ and Phosphate Buffered Saline (PBS). Here, we describe accelerated aneurysm formation resulting from a modification of the $CaCl_2$ model.

**Methods—**The modified $CaCl_2$, the $CaPO_4$ model, was created by applying PBS onto the mouse infrarenal aorta after $CaCl_2$ treatment. Morphological, histological and immunohistochemical analyses were performed on arteries treated with both the $CaPO_4$ model and the conventional $CaCl_2$ model as control. *In vitro* methods were carried out using a mixture of $CaCl_2$ and PBS to create $CaPO_4$ crystals. $CaPO_4$ induced apoptosis of primary cultured mouse vascular smooth muscle cells (VSMCs) was measured by DNA fragmentation ELISA.

**Results—**First, we showed that the $CaPO_4$ model produces AAA, defined as an increase of 50% or greater in the diameter of the aorta; faster than in the $CaCl_2$ model. $CaPO_4$ model showed significantly larger aneurysmal dilation at 7, 28, and 42 days as reflected by a maximum diameter fold change (measured in mm) of 1.69 ± 0.07, 1.99 ± 0.14 and 2.13 ± 0.09 as opposed to 1.22 ± 0.04, 1.48 ± 0.07 and 1.68±0.06 as seen in $CaCl_2$ model, respectively (n=6; $P<0.05$). A semi-quantitative grading analysis of elastin fiber integrity at 7 days revealed a significant increase in elastin degradation in the CaPO4 model as compared to $CaCl_2$ model (2.7±0.2 vs 1.5±0.2, $p<0.05$, n=6). Significantly higher level of apoptosis occurred in the $CaPO_4$ model (apoptosis index at 1, 2, and 3 days post-surgery: 0.26 ± 0.14, 0.37± 0.14, and 0.33 ± 0.08 for $CaPO_4$ model and 0.012 ± 0.10, 0.15± 0.02, and 0.12 ± 0.05 for conventional $CaCl_2$ model) (n=3; $p<0.05$). An enhancement of macrophage infiltration and calcification was also observed at 3 and 7 days in $CaPO_4$. $CaPO_4$ induced approximately 3.7 times more apoptosis in VSMCs when compared to a mixture of $CaCl_2$ (n=4; $p<0.0001$) *in vitro*.

**Conclusion—**Our data shows that the $CaPO_4$ model accelerates aneurysm formation with the enhancement of apoptosis, macrophage infiltration and calcium deposition. This modified model, with its rapid and robust dilation, can be utilized as a new model for AAA.

[†]All Correspondence to: Bo Liu, PhD, 1111 Highland Avenue, Madison, WI 53792, Tel: 608-263-5931, Fax: 608-265-1102, liub@surgery.wisc.edu.
[*]Equally contributed to this manuscript

This manuscript is being presented at the 2011 Midwestern Vascular Annual Meeting.

## Introduction

Abdominal aortic aneurysm (AAA) is a common vascular disease associated with high mortality. Aneurysm results from the culmination of a series of events that lead to disruption of structural integrity and segmental weakening of the abdominal aortic wall. AAA is the 10th leading cause of death in men over the age of fifty-five and claims as many as 30,000 deaths each year in the US[1]. It is estimated that the prevalence of AAA increases continuously in men over the age of 55 and reaches a peak of more than 10% in those 80 to 85 years old[2].

Several animal models have been created to aid investigation of pathophysiological events underlying human AAA, including models dependent upon genetic and/or chemical manipulation[3]. Genetic manipulations are often associated with defects in extracellular matrix maturation, disruption of lipid homeostasis, or alteration of angiotensin enzymes[4–7]. The chemically-induced aneurysm approaches include the intraluminal infusion of elastase and the periaortic application of calcium chloride ($CaCl_2$). A third chemical approach combines chemical and genetic approaches, using a systemic infusion of angiotensin II to mice genetically altered to compromise lipid homeostasis such as mice deficient in Apolipoprotein E (Apo E) or Low Density Lipoprotein (LDL) receptor[8–11].

Aneurysmal changes in the carotid artery of hyperlipidemic rabbits resulting from periaortic application of $CaCl_2$ was first described by Gertz, SD et al[12]. This method was later applied in the abdominal aortas of hyperlipidemic rabbits in combination with thioglycollate, as reported by Freestone et al[13] and subsequently adapted to mice [10, 14]. Typically, by applying$CaCl_2$ soaked gauze to the infrarenal aorta for 15–20 minutes, one can reproducibly generate a aneurysmal dilationdilation in the treated aortic segment within 4–6 weeks[14, 15]. This model does not require the use of genetically modified mice. Similar to the elastase-induced mouse aneurysm, $CaCl_2$-induced aneurysmal dilationdilation is accompanied by the depletion of medial layer smooth muscle cells, as well as elastin degradation, infiltration of lymphocytes and macrophages, elevation of pro-inflammatory cytokines and the increased activation of matrix metalloproteinases (MMPs) [10, 14, 15].

The mechanism by which adventitial application of $CaCl_2$ causes the above described molecular and cellular changes in the aortic wall is not entirely clear. Previous findings have identified calcium ion binding sites on both collagen and elastin, suggesting that $CaCl_2$ application may facilitate the degradation of these major arterial structure components[16]. Our own group has identified significant calcification also occurring in $CaCl_2$-treated arteries, mainly in the medial layer. We hypothesized that this calcification may also contribute to aneurysm formation, and explored the formation of these calcification deposits. Calcium phosphate ($CaPO_4$) crystals have been identified as the major component of calcification found in atherosclerosis[17–19], and have been suggested to have significant proinflammatory effects, induce apoptosis in various cell types, and stimulate production of pro-inflammatory cytokines from monocytes/macrophages and smooth muscle cells (SMCs)[20, 21].

In the current study, we tested whether calcium phosphate is a more potent stimulus than calcium chloride in stimulation of apoptosis and induction of inflammatory cytokines. Based on the $CaPO_4$ based cell transfection method, we adapted a method of calcium phosphate generation *in vivo* through a sequential application of $CaCl_2$ and phosphate buffered saline (PBS).[22–24] Compared to application of $CaCl_2$ alone, the sequential application of $CaCl_2$ and PBS produces a more severe, rapid dilationdilation of the aneurysmal artery associated with significantly enhanced smooth muscle apoptosis and inflammatory responses. While future studies are necessary to determine how this new method, termed the $CaPO_4$ model,

may cause arterial injury, its rapid induction of aneurysmal dilation is advantageous and could be used as an additional rodent model in studies of AAA.

## Materials and Methods

### General Materials

Dulbecco's Modified Eagles Medium (DMEM) and cell culture reagents were from Gibco BRL Life Technologies. Chemicals, if not specified, were purchased from Sigma Chemical Co.

### Mouse Models of AAA

Male C57BL/6 mice, 12 weeks of age, were purchased from Jackson Laboratory (Bar Harbor, ME). All mice had free access to a normal diet and water. $CaPO_4$ induced abdominal aortic aneurysm model were created through a method closely resembling the $CaCl_2$ induced model as described by Gertz et al.[25] Under the general anesthesia, midline incision was made and the infrarenal region of the abdominal aorta was isolated. A small piece of gauze soaked in 0.5M $CaCl_2$ was applied perivascularly for 10 minutes. This gauze is then replaced with another piece of phosphate buffered saline (PBS)-soaked gauze for 5 minutes. $CaCl_2$ induced aneurysm was created through a similar manner but with a single treatment of 0.5M $CaCl_2$ soaked gauze for 15 minutes. Histological analyses suggest that vascular injury appears to be more severe at the anterior surface where arterial tissue comes in contact with gauzes. Control mice received a single treatment of 0.5M Sodium Chloride (NaCl) soaked gauze for 15 minutes. The maximum external diameter of the infrarenal aorta was measured using a digital caliper (VWR Scientific, Radnor, PA) prior to treatment and at the time of tissue harvest. At selected time points, mice were sacrificed and tissues were perfusion-fixed with a mixture of 4% paraformaldehyde (PFA) in PBS at physiological perfusion pressure. Harvested tissue was further fixed in 4% PFA and imbedded in O.C.T. Compound (Sakura Tissue Tek, Netherlands). All sections were cut 6μm thick using a Leica CM3050S cryostat. All animal procedures were conducted in accordance with experimental protocols that were approved by the Institutional Animal Care and Use Committee at the University of Wisconsin, Madison (Protocol M02284).

### Histology and Immunohistochemistry

Van Geison stains were carried out using Chromaview Van Gieson kit (Richard Allan Scientific, Kalamazoo, MI) according to provided protocol. Elastin integrity was quantified using a grading system as described by Kitamonto et al: (1, no elastin degradation or mild elastin degradation; 2, moderate; 3, moderate to severe; and 4, severe elastin degradation).[26] Each section was numbered and photographed at 10x or 20x magnification, maintaining their respective numbers. Then, an objective participant graded the photographs according to the aforementioned scale and recorded the grade with the section number. Calcification was detected using Alizarin Red (Ricca Chemical Company; Arlington, TX). Quantification of calcium content was calculated using ImageJ Software as provided by the National Institutes of Health. Total area of calcified media (stained red) was calculated and divided by total medial area of the artery to yield the reported ratio(s).

For additional immunohistochemistry, arterial sections were permeabilized with 0.1% TritonX for 10 minutes at room temperature. Non-specific sites were blocked using 5% bovine serum albumin (BSA), 3% normal donkey serum in Tris-buffered Saline and Tween 20 (TBS-T) for 1 hour at room temperature. Primary antibodies to CD3, MCP-1, and Mac3 were purchased from Santa Cruz (Santa Cruz, CA), MOMA2 was purchased from Abcam (Cambridge, MA), Cleaved Caspase 3 (CC3) was purchased from Cell Signaling Technology (Boston, MA), and Smooth muscle alpha-actin (SMA) was purchased from

Sigma-Aldrich (St. Louis, MO). Primary antibodies were diluted in previously described blocking solution and incubated overnight at 4°C. Apoptosis was identified through Terminal deoxynucleotidyl transferase dUTP nick end labeling (TUNEL) in an *In Situ* Cell Death Detection Kit (Roche, Indianapolis, IN), carried out according to kit directions. Fluorescent stains were completed using secondary antibodies purchased from Invitrogen Molecular Probes (Carlsbad, CA) and 4′6-diamidino-2-phenyl-indole, dihydrochloride (DAPI, Invitrogen, Carlsbad, CA) was used to detect nuclei. Staining was visualized with a Nikon Eclipse E600 upright microscope and digital images were acquired using a RetigaEXi CCD digital camera. Quantification of stains was performed in a manner to that previously described [27] using Image J Software. Data quantification was performed using at least 3 sections per artery.

## Cell Culture

Primary mouse aortic SMCs from the aorta of C57BL/6 mice were isolated based on a protocol described by Clowes et al [28]. Briefly, aortas were perfused with PBS supplemented with 2% penicillin/streptavidin antibiotics. The aorta was isolated from the aortic arch to the iliac bifurcation and incubated 30 minutes in digestion buffer at 37°C. Adventitia was pulled away from the medial layer, tissues were minced, and further incubated for 4 hours at 37°C. Cells isolated from medial layer of individual mice were kept in separate dishes to allow a biological replicate from each animal. Tissue was spun to a pellet by centrifugation and washed with 10% FBS DMEM once, then suspended in a small volume of 10%FBS-DMEM and left undisturbed for 48 hours to allow cells to migrate from tissue. All cell types were maintained in DMEM supplemented with 10% fetal calf serum (FCS), 100 units/mL penicillin, and 100μg/mL streptomycin in a 5% $CO_2$/water-saturated incubator at 37°C.

## In vitro $CaCl_2$ and $CaPO_4$ Treatments

10% FBS DMEM was replaced with 0.5% FBS DMEM 24 hours prior to all cell treatment. Cells designated for $CaCl_2$ treatment were washed with normal saline twice before being treated with $CaCl_2$ (final concentration 0.05M) diluted in normal saline. Treated cells were incubated at 37°C for 15 minutes, $CaCl_2$ solution was removed and cells were washed twice with 10%FBS DMEM and let rest 6 hours at 37°C. Cells designated for $CaPO_4$ treatment were washed twice with 1x PBS before being treated with $CaCl_2$ (final concentration 0.05M) diluted in 1x PBS for 15 minutes. The remainder of the treatment method was the same as the $CaCl_2$ group.

## DNA Fragmentation ELISA

*In vitro* detection of apoptosis via fragmented DNA labeling was carried out using the Cell Death Detection ELISA kit (Roche, Indianapolis, Indiana) according to manufacturer's protocol.

## Flow Cytometric Analysis

Apoptotic populations in treated cell groups were assessed by flow cytometry using a PE Annexin V Apoptosis Detection Kit (BD Pharmigen, San Diego, CA). Flow cytometric data was collected on a BD FACS Calibur Flow Cytometer equipped with a Cytek 633nm laser (Freemont, CA) and analysis was performed using Flow Jo software (TreeStar, Inc.).

## Statistical analysis

Values were expressed as means ± standard error. Experiments were repeated at least three times unless stated otherwise. Differences between 2 groups were analyzed by Student's t test, and one-way analysis of variance (ANOVA) followed by Scheffe's test was used for multiple comparisons. Values of $P<0.05$ were considered significant.

## Results

### Calcium phosphate induces apoptosis in aortic SMCs

Primary cultured mouse aortic SMCs were treated with either $CaCl_2$ or $CaPO_4$; control SMCs were similarly treated with normal saline. At the end of treatment, cells were placed into normal growth media for 6 hours before being subjected to apoptotic evaluation. Analyses of DNA fragmentation indicated the presence of apoptotic cells in both $CaCl_2$- and $CaPO_4$-treated cells, however, $CaPO_4$ induced approximately 3.7 times more apoptosis of SMCs compared to $CaCl_2$ ($P<0.0001$) (Fig. 1A). Detailed cell profiling via FACS analysis showed that the majority of dead cells in the $CaCl_2$-treated group stained positive for both Annexin V and 7 AAD, indicating secondary necrosis. On the other hand, the majority of dead cells in the $CaPO_4$-treated group stained positive only for Annexin V, indicating apoptosis to dominate this treatment group (Fig. 1B and Table 1).

### $CaPO_4$ exacerbates aneurysm formation in mice

To facilitate $CaPO_4$ crystal formation *in vivo*, we sequentially applied $CaCl_2$ and PBS, or $CaCl_2$ alone as a control, to the adventitial surface of mouse abdominal aorta. Mice were sacrificed at designated time points following the injury and the maximum diameter of the aortas was measured. Aneurysm development was assessed by determining the fold change in diameter, calculated as the post-surgical measurement divided by the diameter measured prior to injury. As shown in Fig. 2, the aortas treated by $CaPO_4$ showed significantly larger aneurysmal dilation at 7, 28 and 42 days as reflected by a maximum diameter fold change of $1.69 \pm 0.07$, $1.99 \pm 0.14$ and $2.13 \pm 0.09$ as opposed to $1.22 \pm 0.04$, $1.48 \pm 0.07$ and $1.68 \pm 0.06$ as seen in $CaCl_2$ model, respectively ($n=6$; $P<0.05$) (Fig 2A and B). The van Gieson staining of the aortic wall at day 7 showed more fragmentation of the elastin layer in $CaPO_4$ treated aorta (Fig. 2C). A semi-quantitative grading analysis of elastin fiber integrity at 7 days revealed a significant increase in elastin degradation in the $CaPO_4$ model as compared to $CaCl_2$ model (Fig. 2D).

### Calcium phosphate intensifies apoptosis in aneurysmal arteries

Next, we compared the magnitude of apoptosis following aneurysm induction with either $CaCl_2$ or $CaPO_4$ by harvesting arteries at 1, 2 and 3 days post-injury. Apoptosis in the aortic wall was evaluated by TUNEL staining at each time point. As demonstrated by representative image and graphical depiction, $CaPO_4$ injury induced significantly more apoptosis than $CaCl_2$ injury at 2 and 3 days post-injury (Fig. 3A and B, respectively). Most of the apoptotic cells were noted in the media and localized to cells that were positive for smooth muscle specific alpha actin (SMA) (Supp. Fig. 1).

### Calcium phosphate-induced aneurysm is associated with inflammation and medial calcification

A prevalent feature of human and experimental aneurysms is significant inflammatory infiltrate. We have previously reported a relationship between apoptosis of SMCs and the inflammatory response(s) leading to the infiltration of macrophages and other inflammatory cells to the aortic wall[29]. At this notion, $CaPO_4$-treated arteries were stained for the presence of macrophages, as identified by the marker CD68. Representative images found in Figure 4A depict $CaPO_4$-treated arteries harvested 3 days after injury, showing significant macrophage infiltration. Figure 4B shows graphical representation of macrophage infiltration as determined by CD68 positive cells divided by total nuclei. Supplemental Figure 2 depicts additional inflammatory markers in day 3 $CaPO_4$-treated arteries. Macrophage marker Mac3, T lymphocyte marker CD3, and the inflammatory cytokine monocyte chemoattractant protein-1 (MCP-1) evidenced a significant inflammatory

response. Using cleaved (activated) caspase 3 as a marker for apoptosis, we evaluated the spatial relationship between apoptosis and inflammation. As shown in Supplemental Figure 3 A, monocytes and Macrophages, marked by MOMA, localized mostly in the adventitia. Using cleaved or activated caspase 3 as a marker for apoptosis, we found that the majority of monocytes and macrophages at this time point were not apoptotic, however, they tended to concentrate in areas proximal to apoptotic cells (Supp. Fig. 3).

Significant calcification in $CaPO_4$ treated arteries was easily noted visually and tactilely at the time of artery harvest. Cross sections of the aortas receiving treatment with either $CaCl_2$ or $CaPO_4$ injury were stained with Alizarin Red staining according to manufacturer's protocol. $CaPO_4$ injury caused pronounced medial calcification appearing around 48 hours post-injury, and maximizing around 7 days (Fig. 5A and B).

## Discussion

Animal models of AAA have been utilized in a range of experiments to explore various aspects of AAA pathogenesis as well as potential methods of AAA treatment. Here, we reported the creation of mouse experimental AAA model with rapid and robust aneurysmal dilationdilation through sequential adventitial application of $CaCl_2$ and PBS. This modified $CaCl_2$ model, or the $CaPO_4$ model, displayed similar pathological and histological characteristics as the previously described $CaCl_2$ but at a higher magnitude.

We postulate that adventitial insult in the form of $CaCl_2$ application causes a series of tissue degenerative events, at least in part through formation of $CaPO_4$ crystals. This argument is supported by our finding that $CaCl_2$ did not cause significant degree of apoptosis or necrosis when applied to cultured mouse aortic SMCs. In contrast, cultured mouse aortic SMCs responded to $CaPO_4$ with massive apoptosis, findings consistent with reports from other groups[30–32].

Although the creation of aneurysm phenotype with either $CaCl_2$ or $CaPO_4$ is artificial, atherosclerotic calcification has been shown to consist mainly of $CaPO_4$ crystals, which is typically seen in the intimal and medial layer of the diseased human aorta[1819, 33]. We did observe medial calcification in the arterial segments that sustained the $CaCl_2$ or $CaPO_4$ insult. Although substantial calcification is noted in these arteries by both tactile and immunohistochemical methods, the biological mechanisms underlying this ectopic calcification have yet to be identified. Thus, future studies may lend insight to these processes through identification of calcification regulating genes such as osteopontin.

Interestingly, robust apoptosis and calcification was observed in the medial layer of the aorta starting at around 2 days after surgery, a time point the elastin fibers appeared grossly intact.

A potential causal relationship between apoptosis and calcification has been conceptualized by Proudfoot and colleagues[34], who propose a model in which smooth muscle cell death may form apoptotic bodies in the arterial wall, which in turn may serve as a nucleus for vascular calcification[35]. In our time course studies, we noted the time line of apoptotic induction in the arterial wall, which was noted to begin around 24 hours, was closely followed by the detection of calcium deposition around 48 hours post injury. However, the link between SMC apoptosis and medial calcification has yet to be directly tested. Although aortic calcification has been reported in human AAA[36], the precise contribution calcification may make toward aneurysm progression is still controversial.

One important limitation within this study lies in the formation of $CaPO_4$ crystals. Although these crystals are known to be generated by mixing $CaCl_2$ with phosphate buffer, this methodology provides no means of controlling the formation of $CaPO_4$ crystals, nor of

measuring the final concentration or composition of these crystals, especially *in vivo*. In preliminary studies, we tested the periaortic application of several forms of calcium phosphate including hydroxyapatite, nanocrystal and basic calcium phosphate. However, each of these calcium phosphate forms failed to induce aneurysm formation *in vivo* and produced little if any apoptosis *in vitro*. One possible explanation for this significant difference between calcium phosphate crystal types is size variations amongst these crystals, particularly in comparison to the naturally formed crystals, may not be appropriate for the endocytosis or autophagocytosis of these crystals to induce apoptosis[37, 38]. In order to address a few questions surrounding the role of these $CaPO_4$ crystals, methods of interfering with crystal formation and/or the chemical reaction(s) that take place may provide mechanistic insights. Although the scope of this study does not allow such an experiment, future work must explore these methods in order to fully understand the role of $CaPO_4$ crystals in this newly described model. Furthermore, a better understanding of the role of calcification in aneurysm is necessary to fully understand the potential impact of this study.

## Conclusion

In conclusion, we have shown that the creation of a $CaPO_4$ mouse AAA model through the modification of the conventional $CaCl_2$ model significantly accelerates aneurysm formation. $CaPO_4$ treatment also induced significant enhancement of apoptosis both *in vitro* and *in vivo*. Calcification and macrophage infiltration were also prominent features of the $CaPO_4$ aneurysm, sharing spatial and temporal similarities to the apoptosis within the medial layer. This model, with its rapid and robust dilationdilation, can be utilized as a new model for mouse experimental AAA.

## Supplementary Material

Refer to Web version on PubMed Central for supplementary material.

## Acknowledgments

**Funding**

This work was supported by the National Institute of Health R01HL088447 (BL and KCK), American Heart Association 10GRNT3020052 (BL and SM) and Howard Hughes Medical Institute MSN135276 (SS).

## References

1. Kent KC, Zwolak RM, Jaff MR, Hollenbeck ST, Thompson RW, Schermerhorn ML, Sicard GA, Riles TS, Cronenwett JL. Screening for abdominal aortic aneurysm: A consensus statement. J Vasc Surg. 2004; 39:267–269. [PubMed: 14718853]
2. Bengtsson H, Sonesson B, Bergqvist D. Incidence and prevalence of abdominal aortic aneurysms, estimated by necropsy studies and population screening by ultrasound. Ann N Y Acad Sci. 1996; 800:1–24. [PubMed: 8958978]
3. Daugherty A, Cassis LA. Mouse models of abdominal aortic aneurysms. Arterioscler Thromb Vasc Biol. 2004; 24:429–434. [PubMed: 14739119]
4. Brophy CM, Tilson JE, Braverman IM, Tilson MD. Age of onset, pattern of distribution, and histology of aneurysm development in a genetically predisposed mouse model. J Vasc Surg. 1988; 8:45–48. [PubMed: 3385878]
5. Silence J, Collen D, Lijnen HR. Reduced atherosclerotic plaque but enhanced aneurysm formation in mice with inactivation of the tissue inhibitor of metalloproteinase-1 (timp-1) gene. Circ Res. 2002; 90:897–903. [PubMed: 11988491]
6. Kuhlencordt PJ, Gyurko R, Han F, Scherrer-Crosbie M, Aretz TH, Hajjar R, Picard MH, Huang PL. Accelerated atherosclerosis, aortic aneurysm formation, and ischemic heart disease in

apolipoprotein e/endothelial nitric oxide synthase double-knockout mice. Circulation. 2001; 104:448–454. [PubMed: 11468208]

7. Nishijo N, Sugiyama F, Kimoto K, Taniguchi K, Murakami K, Suzuki S, Fukamizu A, Yagami K. Salt-sensitive aortic aneurysm and rupture in hypertensive transgenic mice that overproduce angiotensin ii. Lab Invest. 1998; 78:1059–1066. [PubMed: 9759650]
8. Anidjar S, Salzmann JL, Gentric D, Lagneau P, Camilleri JP, Michel JB. Elastase-induced experimental aneurysms in rats. Circulation. 1990; 82:973–981. [PubMed: 2144219]
9. Curci JA, Thompson RW. Variable induction of experimental abdominal aortic aneurysms with different preparations of porcine pancreatic elastase. J Vasc Surg. 1999; 29:385. [PubMed: 9950998]
10. Chiou AC, Chiu B, Pearce WH. Murine aortic aneurysm produced by periarterial application of calcium chloride. J Surg Res. 2001; 99:371–376. [PubMed: 11469913]
11. Daugherty A, Manning MW, Cassis LA. Angiotensin ii promotes atherosclerotic lesions and aneurysms in apolipoprotein e-deficient mice. J Clin Invest. 2000; 105:1605–1612. [PubMed: 10841519]
12. Gertz SD, Kurgan A, Eisenberg D. Aneurysm of the rabbit common carotid artery induced by periarterial application of calcium chloride in vivo. J Clin Invest. 1988; 81:649–656. [PubMed: 3343336]
13. Freestone T, Turner RJ, Higman DJ, Lever MJ, Powell JT. Influence of hypercholesterolemia and adventitial inflammation on the development of aortic aneurysm in rabbits. Arterioscler Thromb Vasc Biol. 1997; 17:10–17. [PubMed: 9012631]
14. Longo GM, Xiong W, Greiner TC, Zhao Y, Fiotti N, Baxter BT. Matrix metalloproteinases 2 and 9 work in concert to produce aortic aneurysms. J Clin Invest. 2002; 110:625–632. [PubMed: 12208863]
15. Yoshimura K, Aoki H, Ikeda Y, Fujii K, Akiyama N, Furutani A, Hoshii Y, Tanaka N, Ricci R, Ishihara T, Esato K, Hamano K, Matsuzaki M. Regression of abdominal aortic aneurysm by inhibition of c-jun n-terminal kinase. Nat Med. 2005; 11:1330–1338. [PubMed: 16311603]
16. Urry DW. Neutral sites for calcium ion binding to elastin and collagen: A charge neutralization theory for calcification and its relationship to atherosclerosis. Proc Nat Acad Sci USA. 1971; 68:810–814. [PubMed: 4251554]
17. Bostrom K, Watson KE, Stanford WP, Demer LL. Atherosclerotic calcification: Relation to developmental osteogenesis. Am J Cardiol. 1995; 75:88B–91B. [PubMed: 7801876]
18. Weissen-Plenz G, Nitschke Y, Rutsch F. Mechanisms of arterial calcification: Spotlight on the inhibitors. Adv Clin Chem. 2008; 46:263–293. [PubMed: 19004192]
19. Villa-Bellosta R, Sorribas V. Calcium phosphate deposition with normal phosphate concentration. Circ J. 2011
20. Ewence AE, Bootman M, Roderick HL, Skepper JN, McCarthy G, Epple M, Neumann M, Shanahan CM, Proudfoot D. Calcium phosphate crystals induce cell death in human vascular smooth muscle cells: A potential mechanism in atherosclerotic plaque destabilization. Circ Res. 2008; 103:e28–34. [PubMed: 18669918]
21. Pazar B, Ea HK, Narayan S, Kolly L, Bagnoud N, Chobaz V, Roger T, Liote F, So A, Busso N. Basic calcium phosphate crystals induce monocyte/macrophage il-1beta secretion through the nlrp3 inflammasome in vitro. J Immunol. 2011; 186:2495–2502. [PubMed: 21239716]
22. Graham FL, van der Eb AJ. A new technique for the assay of infectivity of human adenovirus 5 DNA. Virology. 1973; 52:456–467. [PubMed: 4705382]
23. Jordan M, Wurm F. Transfection of adherent and suspended cells by calcium phosphate. Methods. 2004; 33:136–143. [PubMed: 15121168]
24. Wilson SP, Liu F, Wilson RE, Housley PR. Optimization of calcium phosphate transfection for bovine chromaffin cells: Relationship to calcium phosphate precipitate formation. Analytical Biochemistry. 1995; 226:212–220. [PubMed: 7793620]
25. Gertz SD, Kurgan A, Eisenberg D. Aneurysm of the rabbit common carotid artery induced by periarterial application of calcium chloride in vivo. The Journal of Clinical Investigation. 1988; 81:649–656. [PubMed: 3343336]

26. Kitamoto S, Sukhova GK, Sun J, Yang M, Libby P, Love V, Duramad P, Sun C, Zhang Y, Yang X, Peters C, Shi G-P. Cathepsin l deficiency reduces diet-induced atherosclerosis in low-density lipoprotein receptor–knockout mice. Circulation. 2007; 115:2065–2075. [PubMed: 17404153]
27. Tang XN, Berman AE, Swanson RA, Yenari MA. Digitally quantifying cerebral hemorrhage using photoshop® and image j. Journal of Neuroscience Methods. 2010; 190:240–243. [PubMed: 20452374]
28. Clowes A, Clowes M, Fringerle J, Reidy M. Kinetics of cellular poliferation after arterial injury: Role of acute distension in the induciton of smooth muscle proliferation. Lab Invest. 1989; 60:360–364. [PubMed: 2927077]
29. Yamanouchi D, Morgan S, Kato K, Lengfeld J, Zhang F, Liu B. Effects of caspase inhibitor on angiotensin ii-induced abdominal aortic aneurysm in apolipoprotein e-deficient mice. Arterioscler Thromb Vasc Biol. 2010; 30:702–707. [PubMed: 20075419]
30. Ewence AE, Bootman M, Roderick HL, Skepper JN, McCarthy G, Epple M, Neumann M, Shanahan CM, Proudfoot D. Calcium phosphate crystals induce cell death in human vascular smooth muscle cells. Circulation Research. 2008; 103:e28–e34. [PubMed: 18669918]
31. Pazár B, Ea H-K, Narayan S, Kolly L, Bagnoud N, Chobaz V, Roger T, Lioté F, So A, Busso N. Basic calcium phosphate crystals induce monocyte/macrophage il-1β secretion through the nlrp3 inflammasome in vitro. The Journal of Immunology. 2011; 186:2495–2502. [PubMed: 21239716]
32. Trion A, van der Laarse A. Vascular smooth muscle cells and calcification in atherosclerosis. American Heart Journal. 2004; 147:808–814. [PubMed: 15131535]
33. Hunt JL, Fairman R, Mitchell ME, Carpenter JP, Golden M, Khalapyan T, Wolfe M, Neschis D, Milner R, Scoll B, Cusack A, Mohler ER 3rd. Bone formation in carotid plaques: A clinicopathological study. Stroke. 2002; 33:1214–1219. [PubMed: 11988593]
34. Proudfoot D, Skepper JN, Hegyi L, Bennett MR, Shanahan CM, Weissberg PL. Apoptosis regulates human vascular calcification in vitro: Evidence for initiation of vascular calcification by apoptotic bodies. Circulation Research. 2000; 87:1055–1062. [PubMed: 11090552]
35. Reynolds JL, Joannides AJ, Skepper JN, McNair R, Schurgers LJ, Proudfoot D, Jahnen-Dechent W, Weissberg PL, Shanahan CM. Human vascular smooth muscle cells undergo vesicle-mediated calcification in response to changes in extracellular calcium and phosphate concentrations: A potential mechanism for accelerated vascular calcification in esrd. J Am Soc Nephrol. 2004; 15:2857–2867. [PubMed: 15504939]
36. Matsushita M, Nishikimi N, Sakurai T, Nimura Y. Relationship between aortic calcification and atherosclerotic disease in patients with abdominal aortic aneurysm. Int Angiol. 2000; 19:276–279. [PubMed: 11201598]
37. Sarkar S, Korolchuk V, Renna M, Winslow A, Rubinsztein DC. Methodological considerations for assessing autophagy modulators: A study with calcium phosphate precipitates. Autophagy. 2009; 5:307–313. [PubMed: 19182529]
38. Gao W, Ding WX, Stolz DB, Yin XM. Induction of macroautophagy by exogenously introduced calcium. Autophagy. 2008; 4:754–761. [PubMed: 18560273]

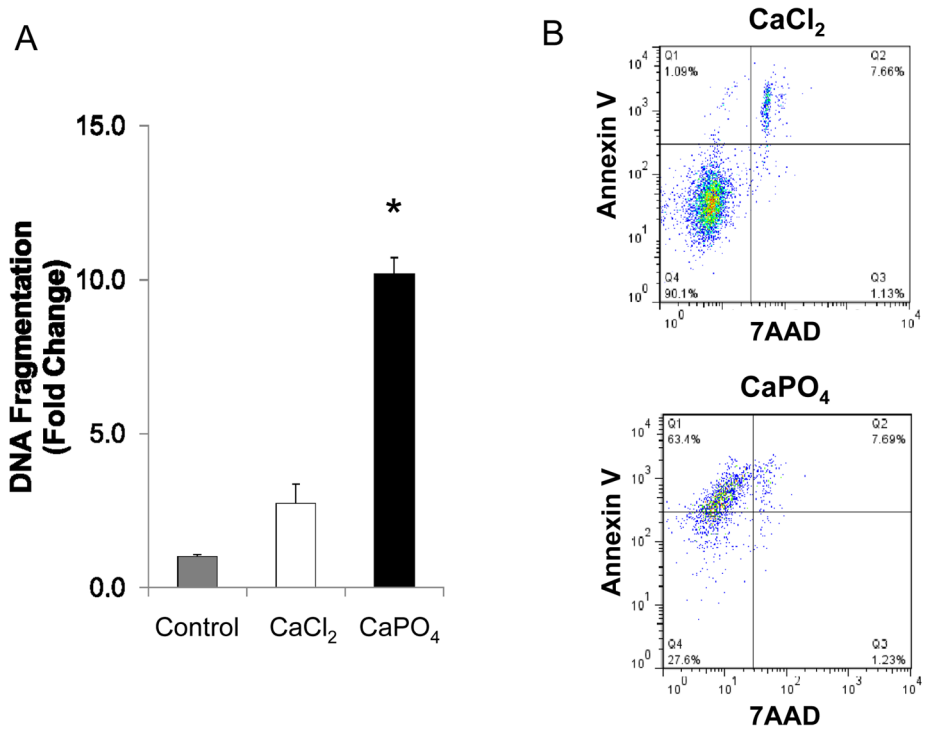


**Figure 1. Apoptosis induced by Calcium phosphate treatment *in vitro***

Cultured mouse aortic SMCs were treated with $CaCl_2$ or $CaPO_4$ as described in Materials and Methods. A) In vitro apoptosis determined by DNA fragmentation ELISA. Fold change determined with comparison to untreated cell group (Control). **p<0.0001, n=**4***. B) Representative results of flow cytometry analyses. Apoptotic and necrotic cells were identified by annexin V and 7AAD, respectively. *n=4.*

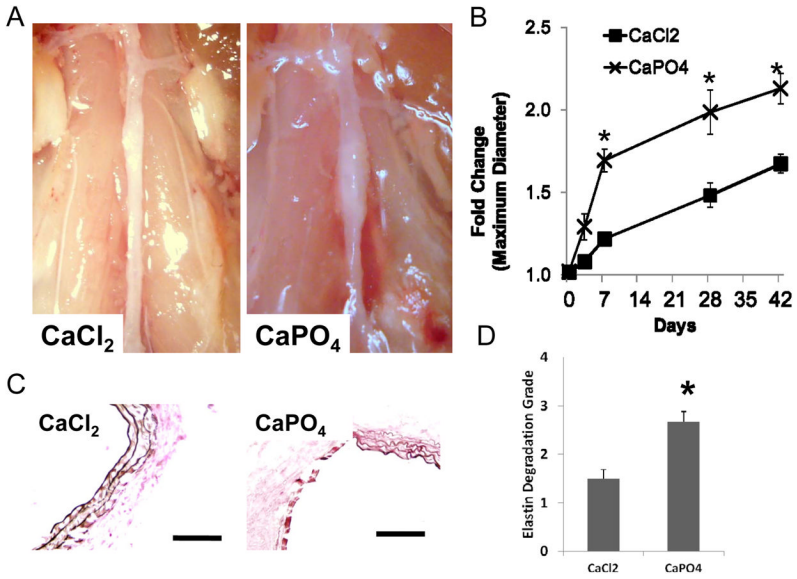


**Figure 2. Aneurysm induction by $CaPO_4$ treatment in mouse model**

Mice were subjected to AAA induction with $CaCl_2$ or $CaPO_4$ and were sacrificed at indicated time points as described in Materials and Methods. A) Representative pictures of arterial dilation 7 days after surgery. B) Quantification of arterial expansion measured 3, 7, 28, and 42 days after surgery. Fold Change = Maximum Diameter/Pre-surgery diameter. *$p < 0.05$, $n = 6$. C) Van Gieson's stain depicting elastin layer degradation in representative treated arteries 7 days after surgery. Scale bar 1003m. D) Semi-quantification of elastin degradation in arteries harvested 7 days after surgery.

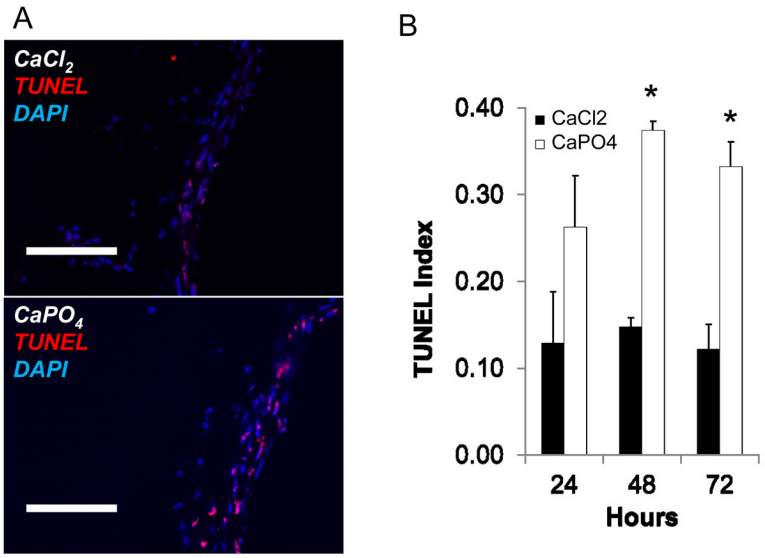


**Figure 3. $CaPO_4$-induced aneurysm displays apoptosis**

Mice were subjected to AAA induction with $CaCl_2$ or $CaPO_4$ and were sacrificed at indicated time points as described in Materials and Methods. A) Representative images of immunohistochemistry for apoptosis, as measured by TUNEL (red), nuclei shown by DAPI stain (blue) in treated arteries 3 days after injury. Scale bar = 100 μm. B) TUNEL index as determined by TUNEL positive cells/nuclei. Measurements taken from $CaCl_2$- (black bar, ■$CaCl_2$) and $CaPO_4$ –treated (white bars, □$CaPO_4$) arteries harvested 24, 48 or 72 hours after surgery. *$p < 0.05$, $n = 3$.

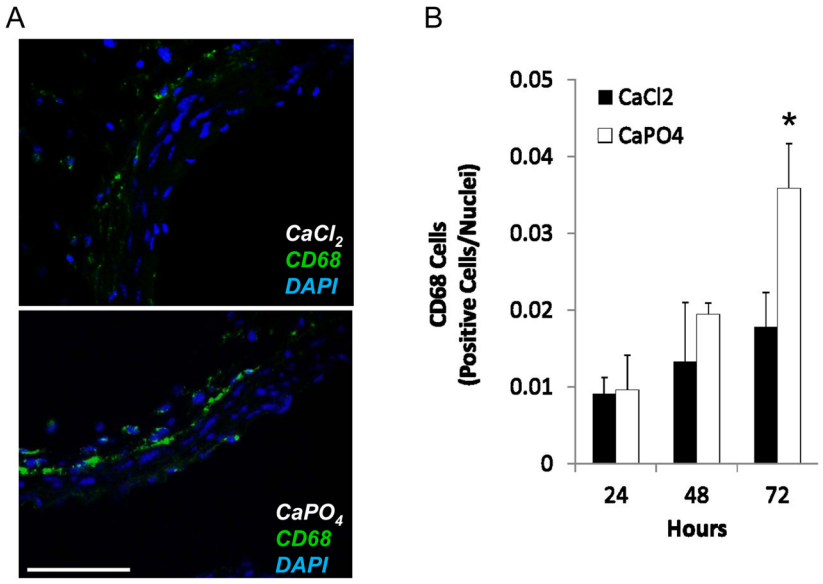


**Figure 4. Inflammation accompanies $CaPO_4$-induced aneurysm**

Mice were subjected to AAA induction with $CaCl_2$ or $CaPO_4$ and were sacrificed at indicated time points as described in Materials and Methods. A) Representative images of immunohistochemistry for macrophage marker CD68 (green) in $CaCl_2$ - and $CaPO_4$ -treated aorta 3 days after injury. Nuclei stained with DAPI (blue). Scale bar = 100 μm. B) Graphical representation of macrophage infiltration as determined by CD68 positive cells/nuclei in treated arteries 24, 48, and 72h after treatment.. *$*p < 0.05, n = 3$.*

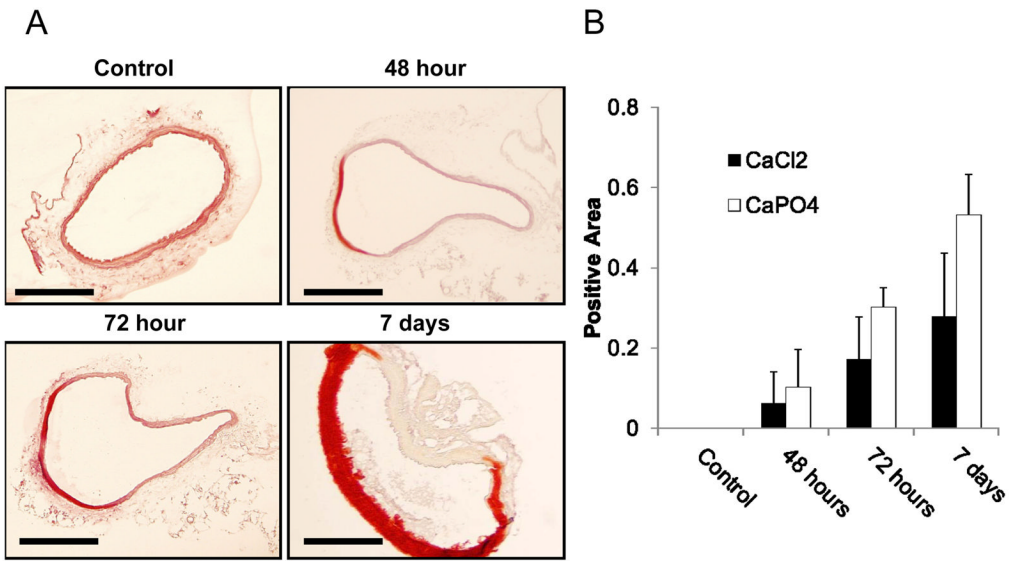


**Figure 5. $CaPO_4$-induced aneurysm samples contain medial calcification**

A) Arterial sections stained with Alizarin Red for calcium deposit detection, calcium appearing red on a pink and yellow background. 'Control' sections harvested from animals treated with NaCl only; '48 hour',' 72 hour', and '7 day' sections harvested at respective times after treatment by $CaPO_4$ surgery. Scale bar = 200 μm for all images. B) Quantification of calcium content in arterial sections harvested from arteries with the conventional $CaCl_2$ model (CaCl2) or the $CaPO_4$ model (CaPO4). Data was expressed as a ratio of the total calcified media divided by the total medial area of each arterial section. *n=4*.

## Table 1

Analysis of cells after treatment with calcium chloride ($CaCl_2$) or calcium phosphate ($CaPO_4$) shown as % of total.

| | Healthy (Negative) | Apoptotic (Annexin V+) | Necrotic (7AAD+) | Secondary necrotic (Double +) |
|---|---|---|---|---|
| $CaCl_2$ | 89.2 ± 1.27 | 1.08 ± 0.01 | 2.79 ± 2.35 | 6.94 ± 1.02 |
| $CaPO_4$ | 22 ± 7.92[a] | 68.8 ± 7.6[a] | 1.4 ± 0.23 | 7.8 ± 0.14 |

*7AAD,* 7-aminoactinomycin D.

[a] $P < 0.05$ vs control.